

High field Mossbauer spectroscopy applied to paramagnetic compounds as a method of selective susceptibility measurement

This article has been downloaded from IOPscience. Please scroll down to see the full text article.

1990 J. Phys.: Condens. Matter 2 4243

(<http://iopscience.iop.org/0953-8984/2/18/020>)

View [the table of contents for this issue](#), or go to the [journal homepage](#) for more

Download details:

IP Address: 171.66.16.103

The article was downloaded on 11/05/2010 at 05:54

Please note that [terms and conditions apply](#).

High field Mössbauer spectroscopy applied to paramagnetic compounds as a method of selective susceptibility measurement

J M Greneche[†], J Linares^{†‡} and F Varret[§]

[†] Laboratoire de Physique des Matériaux, URA CNRS No 807 Faculté des Sciences, 72017 Le Mans Cédex, France

[‡] Departamento de Fisica, Pontificia Universidad Catolica, Lima, Peru

[§] Departement de Recherches Physiques, LA CNRS No 71 Université Pierre et Marie Curie, 75252 Paris Cédex 05, France

Received 20 April 1989, in final form 12 December 1989

Abstract. High field Mössbauer spectroscopy provides a selective method of measurement of the magnetic susceptibility due to paramagnetic Mössbauer atoms, and is well adapted for isotropic ions. This method was successfully tested on crystalline KFeF_4 above its Néel temperature. In the case of $\text{MnFeF}_5(\text{H}_2\text{O})_2$, a reversal of the susceptibility of the iron sublattice was observed near 145 K, and explained in agreement with previous data on the magnetic interactions.

1. Introduction

Several review papers have been devoted to high field Mössbauer spectroscopy (HFMS) showing the various applications of the method (Chappert 1974, Chappert *et al* 1979) or dealing with the computational aspects (Varret 1982). For magnetically ordered systems, it can be an excellent tool for determining the type of magnetic structure for both crystalline and amorphous systems; recent significant examples can be found in Varret *et al* (1982) and Greneche *et al* (1988a).

For paramagnetic compounds, HFMS can provide useful information:

(i) on the sign and sometimes the orientation of the electric field gradient (EFG) and on the asymmetry parameter η (see, for example, Czjzek 1982, Le Caer *et al* 1984, Maurer *et al* 1985);

(ii) on the magnetic hyperfine interaction which is of major interest for investigating the electronic structure of magnetically diluted systems such as biomolecules and coordination complexes (see, for example, Varret and Jehanno 1975, Spertalian and Lang 1980, Spertalian 1983, Huynh *et al* 1983, Mariot *et al* 1983, 1986).

In the case of disordered paramagnetic systems, the situation can be complex, and may involve EFG distributions, as well as exchange interaction distributions which in turn lead to inhomogeneously induced hyperfine fields (Greneche *et al* 1988c).

Here we describe a new kind of application to paramagnets containing isotropic Mössbauer ions among other magnetic ions. The magnetic susceptibility of the

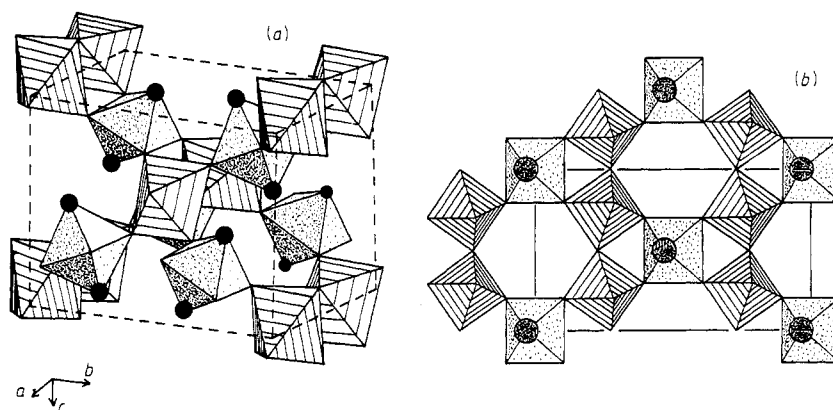


Figure 1. (a) Perspective view of $\text{MnFeF}_5(\text{H}_2\text{O})_2$ structure. The Fe^{3+} octahedra are hatched and the Mn^{2+} octahedra are dotted. The Fe–Fe and Fe–Mn magnetic interactions occur via superexchange M–F–M coupling; the Mn–Mn interactions via the neighbouring water molecules (full circles). (b) Projection of the structure along (011), showing the neighbours in the hexagonal tungsten bronze planes.

Mössbauer ion sublattice (or sublattices) can be separately derived. Such selective information complements the usual susceptibility measurements. We report first on a test of the method on the crystalline ferric fluoride KFeF_4 , and then on selective data on the weberite $\text{MnFeF}_5(\text{H}_2\text{O})_2$ both above their magnetic ordering temperature.

2. Systems under study

The structural and magnetic aspects of the AFeF_4 (with $\text{A} = \text{Rb}, \text{K}, \text{Na}, \text{Cs}$) ferric fluorides have been widely investigated (Heger *et al* 1971, Heger 1972). Their structure consists of layers of tetragonally distorted FeF_6 octahedra separated by A layers. The ferric moments are antiferromagnetically coupled below T_N which is 141 K in the case of KFeF_4 considered here.

$\text{MnFeF}_5(\text{H}_2\text{O})_2$ belongs to the inverse weberite structural type $\text{M}^{2+}\text{Fe}^{3+}\text{F}_5(\text{H}_2\text{O})_2$ (with $\text{M} = \text{Zn}, \text{Mn}, \text{Fe}, \text{Co}, \text{Ni}$) whose aristotype is $\text{Na}_2\text{NiFeF}_7$. Their structure consists of hexagonal tungsten bronze (HTB) planes linked to each other by $\text{M}^{2+}\text{F}_4(\text{H}_2\text{O})_2$ octahedra, as shown in figure 1 (Laligant *et al* 1986). Below the magnetic ordering temperature established at $T_c = 39$ K, $\text{MnFeF}_5(\text{H}_2\text{O})_2$ exhibits a three-dimensional ferrimagnetic frustrated structure which was determined by neutron diffraction (Laligant *et al* 1986) controlled by Mössbauer spectroscopy (Greneche *et al* 1988b); such a behaviour reflects the balance between antiferromagnetic Mn–Mn, Mn–Fe and Fe–Fe interactions.

3. Experimental section

The ^{57}Fe Mössbauer experiments were performed in the transmission geometry using a constant acceleration spectrometer with a ^{57}Co source diffused in a rhodium matrix. The powdered samples were situated in a cryomagnetic system, the applied field direction

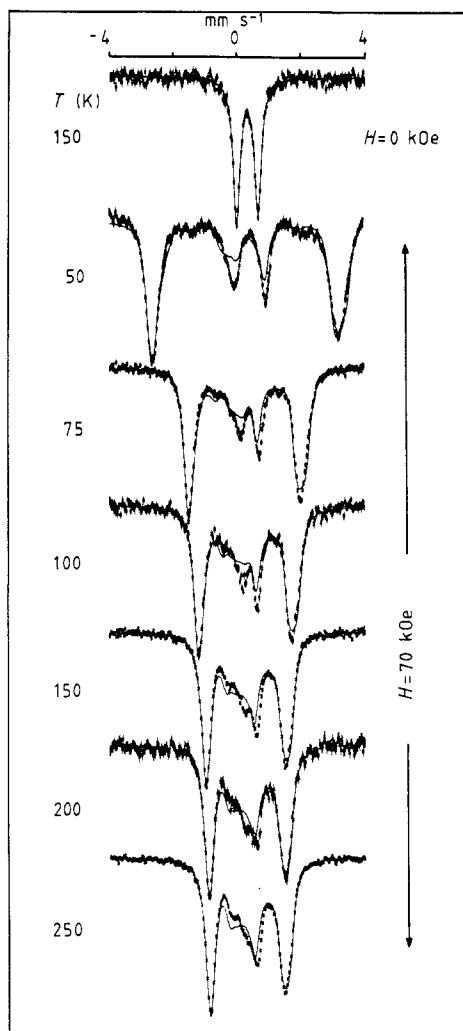


Figure 2. Mössbauer spectra of $\text{MnFeF}_5(\text{H}_2\text{O})_2$ recorded under a 70 kOe applied field parallel to the γ -beam at several temperatures and recorded at 150 K after removal of the applied field.

being parallel to the γ -beam. Several spectra were recorded at temperatures at which the sample is paramagnetic. Since both source and absorber have the same temperature in the cryomagnetic device, the isomer shift (IS) values quoted here do not display the usual thermal effect.

The polycrystalline powder of $\text{MnFeF}_5(\text{H}_2\text{O})_2$ was mixed with vacuum grease in order to hinder the rotation of ferrimagnetic grains under the effect of the external magnetic field; nevertheless we observed, after removal of the field, a weak asymmetry of the quadrupole spectrum due to a very slight texture induced by the application of the magnetic field (Dezsi *et al* 1971), as shown in figure 2. The spectra recorded on KFeF_4 and $\text{MnFeF}_5(\text{H}_2\text{O})_2$ by applying an external magnetic field were classically analysed with the MOSHEX program (see, for instance, Varret 1982). Calibration of the high field spectrometer was performed using a sodium ferrocyanide absorber; we measured the stray field on the Mössbauer source, which was then systematically accounted for when fitting the spectra by computer and taken to be equal to 2 kOe.

Table 1. Hyperfine data on KFeF_4 at several temperatures and the corresponding magnetic susceptibility values deduced from Mössbauer study and obtained from the Faraday method. (IS: isomer shift relative to metallic iron at same temperatures; Γ : linewidth at half height; QS: quadrupole splitting; H_{eff} and H_{hyp} are defined in the text.)

$T \pm 1$ (K)	IS ± 0.01 (mm s ⁻¹)	$\Gamma \pm 0.02$ (mm s ⁻¹)	QS ± 0.05 (mm s ⁻¹)	$H_{\text{eff}} \pm 0.5$ (kOe)	$H_{\text{hyp}} \pm 0.5$ (kOe)	$\chi \pm 0.25 \times 10^{-5}$ (Mössbauer) (emu g ⁻¹)	$\chi \pm 0.05 \times 10^{-5}$ (Faraday) (emu g ⁻¹)
150	0.32	0.37	-1.46	+53.2	-6.8	2.68×10^{-5}	3.22×10^{-5}
175	0.31	0.35	-1.42	+52.1	-7.9	3.09×10^{-5}	3.33×10^{-5}
200	0.31	0.34	-1.43	+51.6	-8.4	3.30×10^{-5}	3.39×10^{-5}
225	0.32	0.34	-1.43	+51.2	-8.8	3.45×10^{-5}	3.40×10^{-5}
250	0.32	0.34	-1.44	+51.1	-8.9	3.48×10^{-5}	3.38×10^{-5}
300	0.32	0.35	-1.43	+51.4	-8.6	3.39×10^{-5}	3.28×10^{-5}

4. Principle of the analysis

A quantitative analysis may be performed on the following basis: in the case of a ferric ion in the ^6S state, the orbital effects, including anisotropic contributions to the hyperfine field and single-ion magnetocrystalline anisotropy, are negligible; the hyperfine field mainly results from the contact interaction which is isotropic. Consequently, both ionic magnetisation and hyperfine field are proportional to the average spin, so

$$H_{\text{hyp}} = (H_{\text{hyp}}(T=0)/m(T=0))m \quad (1)$$

where m is the ion magnetic moment and $H_{\text{hyp}}(T=0)$, $m(T=0)$ refer to the magnetically ordered state, at saturation. The hyperfine field value H_{hyp} is deduced from the measured H_{eff} as follows:

$$H_{\text{eff}} = H_{\text{hyp}} + H_{\text{app}} \quad (2)$$

where these fields are collinear but H_{hyp} is directed oppositely to the magnetisation.

While the magnetic susceptibility χ is defined as the ratio between the magnetisation and the applied field, it finally becomes

$$\chi = (\alpha/M)H_{\text{hyp}}/H_{\text{app}} \quad (3)$$

where M represents the molar mass of the compound under study; in addition, if we wish to express the magnetic susceptibility χ in emu g^{-1} , the coefficient α corresponds to the conversion of typical hyperfine field unit into Bohr magnetons (it has been determined from data obtained at saturation on the crystalline rhombohedral form of the ferric fluoride FeF_3 : $H_{\text{hyp}} = -618$ kOe and $\mu = 4.45 \mu_{\text{B}}$ (Ferey et al 1986)). The sign of the effective field was deduced by continuity from the high temperature range in which the magnetic susceptibility is close to zero.

5. Results for KFeF_4

The spectra recorded over the temperature range 150–300 K, under an external field of 60 kOe have a shape typical for magnetic and quadrupolar interactions of similar magnitudes with a randomly oriented V_{ZZ} direction. The fitted values of the effective field are listed in table 1 while the experimental and the theoretical simulated spectra

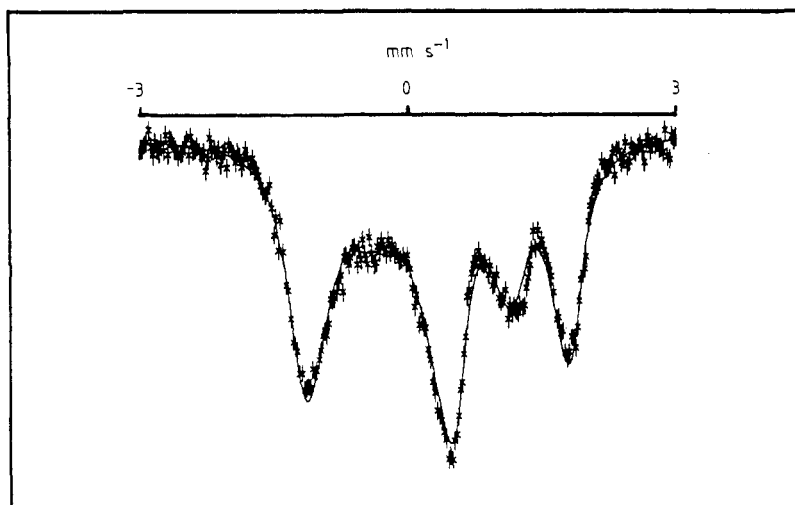


Figure 3. Mössbauer spectrum of powdered KFeF_4 recorded at 150 K under a 60 kOe applied field parallel to the γ -beam.

obtained at 150 K are presented on figure 3. The effective field values are smaller than those of the applied field which is indicative of a positive magnetisation.

The susceptibility data calculated from the present method compare quite well with those directly recorded by the Faraday method, under 10 kOe (also listed in table 1), and are consistent with those obtained by Heger *et al* 1971. However, the Mössbauer value at 150 K is a bit too small. A possible explanation for these small differences is the large value of the applied field, used for Mössbauer experiments, which may induce a non-linear dependence of the magnetisation, mostly near the magnetic ordering temperature.

To summarise, it appears that ^{57}Fe HFMS enables us to measure the magnetic susceptibility of an iron lattice with an accuracy of 10% (except near the magnetic ordering temperature).

6. Results and discussion for $\text{MnFeF}_5(\text{H}_2\text{O})_2$

The Mössbauer spectra recorded under a 70 kOe external field at several temperatures are presented in figure 2; they are typical for a magnetic interaction perturbed by a small random EFG. The theoretical spectra were obtained by considering an isotropic distribution of axial EFG. Some disagreements between the experimental and the simulated spectra can be observed, mainly in the low velocity region where the ratio of the line area intensities is not well reproduced, mostly at low temperatures. Such a discrepancy can be attributed to various and probably combined phenomena: (i) thickness effects which play an important role in the line intensity mainly at low temperatures; (ii) correlations between the distribution of angles θ defined by the main axis V_{ZZ} of the EFG tensor and the γ -beam direction, and the asymmetry parameter of the EFG which is not determined in the weberite case; (iii) the presence of a small quantity of a crystalline impurity like $\text{MnFeF}_5 \cdot 7\text{H}_2\text{O}$ (see Greneche *et al* 1988c). Nevertheless, the effective

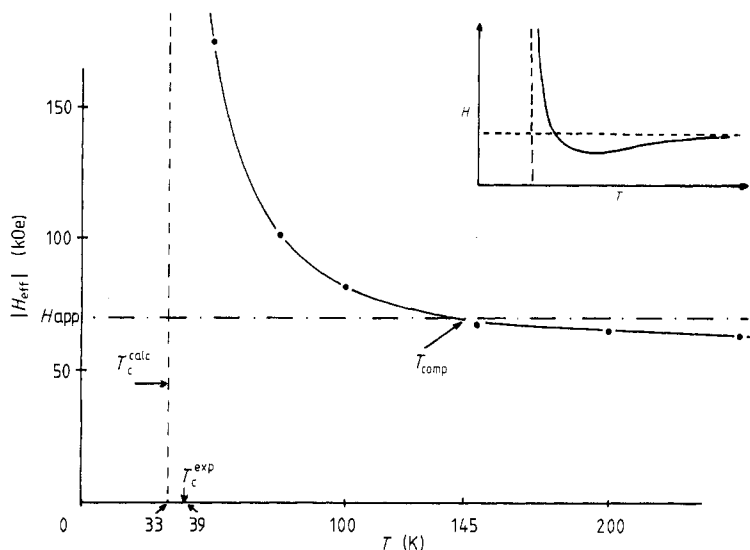


Figure 4. Thermal evolution of the effective field measured from the analysis of the Mössbauer spectra recorded on $\text{MnFeF}_5(\text{H}_2\text{O})_2$ under a 70 kOe applied field. The broken line corresponds to applied field value and the full curve to the theoretical model. Inset: schematic plot on a larger temperature scale.

field measurements, which are the main object of the present study, are thought to be quite accurate since they are generally determined by the most intense lines, which are well reproduced as shown in figure 2.

The effective field data are plotted in figure 4; an interesting ‘compensation’ point occurs at $T_{\text{comp}} = 145 \pm 3 \text{ K}$: the magnetisation of the ferric sublattices reverses, from positive, above T_{comp} , to negative, below T_{comp} . This reveals the increasing influence of the Mn sublattice, which imposes the low temperature magnetisation, according to magnetic data obtained either by neutron diffraction (Laligant *et al* 1986) or by HFMS (Greneche *et al* 1988b).

7. A magnetic model for weberite $\text{MnFeF}_5(\text{H}_2\text{O})_2$

In the present study, we adapt previous calculations in the molecular field approximation (Herpin 1968) to the determination of the partial susceptibility due to iron sublattice.

The paramagnetic susceptibility associated with two magnetic sublattices is easily derived from the usual expressions (Herpin 1968):

$$\mu_{\text{Fe}} = \frac{C_{\text{Fe}}}{T} \left(H_{\text{app}} + n_{\text{Fe}}^{\text{Mn}} \frac{J_{\text{Fe-Mn}}}{\mu_{\text{B}}^2} \mu_{\text{Mn}} + n_{\text{Fe}}^{\text{Fe}} \frac{J_{\text{Fe-Fe}}}{\mu_{\text{B}}^2} \mu_{\text{Fe}} \right) \quad (4)$$

$$\mu_{\text{Mn}} = \frac{C_{\text{Mn}}}{T} \left(H_{\text{app}} + n_{\text{Mn}}^{\text{Fe}} \frac{J_{\text{Fe-Mn}}}{\mu_{\text{B}}^2} \mu_{\text{Fe}} + n_{\text{Mn}}^{\text{Mn}} \frac{J_{\text{Mn-Mn}}}{\mu_{\text{B}}^2} \mu_{\text{Mn}} \right) \quad (5)$$

Table 2. Hyperfine characteristics at several temperatures obtained from Mössbauer spectra recorded on $\text{MnFeF}_5(\text{H}_2\text{O})_2$ under 70 kOe applied field (with symbols defined in table 1).

$T \pm 1$ (K)	$is \pm 0.01$ (mm s ⁻¹)	$qs \pm 0.05$ (mm s ⁻¹)	$H_{\text{eff}} \pm 1$ (kOe)	$H_{\text{hyp}} \pm 1$ (kOe)
50	0.43	0.82	+174.8	+104.8
75	0.42	0.72	+100.7	+30.7
100	0.42	0.70	+81.8	+11.8
150	0.41	0.65	+68.6	-1.4
200	0.41	0.64	+64.7	-5.3
250	0.41	0.64	+63.3	-6.7

where $J_{\text{Fe-Mn}}$, $J_{\text{Fe-Fe}}$ and $J_{\text{Mn-Mn}}$ are respectively the Fe–Mn, Fe–Fe and Mn–Mn exchange integrals, C_{Fe} and C_{Mn} are the Curie constants (they are nearly equal for Mn^{2+} and Fe^{3+}) and $n_{\text{Mn(Fe)}}^{\text{Fe(Mn)}}$ represents the number of Mn (Fe) neighbours of a given Fe (Mn) ion.

Following the crystallographic views presented on figure 1 and considering the superexchange interactions only,

$$n_{\text{Fe}}^{\text{Mn}} = 3 \quad n_{\text{Fe}}^{\text{Fe}} = 3 \quad n_{\text{Mn}}^{\text{Fe}} = 4 \quad n_{\text{Mn}}^{\text{Mn}} = 0.$$

The magnetic configuration then results from the competition between 180° superexchange antiferromagnetic interactions. A more refined model suggested by the complex magnetic structure (see figure 1) accounts for the Mn–Mn super-superexchange interaction through H_2O molecules, with $n_{\text{Mn}}^{\text{Mn}} = 3$.

From equations (4) and (5), one can estimate the paramagnetic susceptibility of iron moments as

$$\begin{aligned} \chi_{\text{Fe}} = & \frac{C_{\text{Fe}}}{T} \left[1 + 3 \frac{J_{\text{Fe-Mn}}}{\mu_{\text{B}}^2} \frac{C_{\text{Mn}}}{T} \left(1 - 3 \frac{C_{\text{Mn}}}{T} \frac{J_{\text{Mn-Mn}}}{\mu_{\text{B}}^2} \right)^{-1} \right] \\ & \times \left[1 - 3 \frac{C_{\text{Fe}}}{T} \frac{J_{\text{Fe-Fe}}}{\mu_{\text{B}}^2} - 12 \left(\frac{J_{\text{Fe-Mn}}}{\mu_{\text{B}}^2} \right)^2 \frac{C_{\text{Fe}}}{T} \frac{C_{\text{Mn}}}{T} \right. \\ & \left. \times \left(1 - 3 \frac{C_{\text{Mn}}}{T} \frac{J_{\text{Mn-Mn}}}{\mu_{\text{B}}^2} \right)^{-1} \right]^{-1}. \end{aligned} \quad (6)$$

This can be expressed as

$$\chi_{\text{Fe}} = C_{\text{Fe}}(T - T_1)/[(T - T_2)(T - T_3)] \quad (7)$$

where T_1 represents the compensation temperature of the iron sublattice

$$T_1 = T_{\text{comp}} = 3(C_{\text{Mn}}/\mu_{\text{B}}^2)(J_{\text{Mn-Mn}} - J_{\text{Fe-Mn}})$$

which is independent of Fe–Fe interactions because the compensation occurs when the iron sublattice is not magnetised.

It can be seen that the values of $T_{2,3}$ are respectively positive and negative in the presence of only antiferromagnetic interactions; so, the larger of T_2 and T_3 is the Curie temperature of the system, i.e. the lowest temperature value for which the Curie approximation can be used. Consequently

$$\begin{aligned} \mu_{\text{B}}^2 T_{\text{c}} = & \frac{3}{2}(C_{\text{Fe}}J_{\text{Fe-Fe}} + C_{\text{Mn}}J_{\text{Mn-Mn}}) + \frac{1}{2}[9(C_{\text{Fe}}J_{\text{Fe-Fe}} + C_{\text{Mn}}J_{\text{Mn-Mn}})^2 \\ & - 12C_{\text{Fe}}C_{\text{Mn}}(3J_{\text{Fe-Fe}}J_{\text{Mn-Mn}} - 4J_{\text{Fe-Mn}}^2)]^{1/2}. \end{aligned}$$

Table 3. Fitted magnetic data in the molecular field model, from the present Mössbauer data.

$n_{\text{Mn}}^{\text{Mn}}$	$J_{\text{Fe-Fe}}$ (K)	$J_{\text{Mn-Mn}}$ (K)	$J_{\text{Mn-Fe}}$ (K)	$C_{\text{Fe,Mn}}^{\dagger}$ (μ_B^2)	T_{comp} (K)	T_c^{\ddagger} (K)
3	-12.50	-1.21	-4.48	15.41	151.2	39§
	-12.53	-1.24	-4.41	15.19	144.5	33
0	-20.38	0§	-3.89	13.21	154.2	39§
	-21.25	0§	-3.78	12.81	145.3	33

† Theoretical value $C_{\text{Fe}} \sim C_{\text{Mn}} = gS(S+1)/3 = 11.67 \mu_B^2$

‡ Experimental Curie temperature = 39 K.

§ Values are fixed when fitting.

The thermal evolution of the effective field measured at different temperatures for $\text{MnFeF}_5(\text{H}_2\text{O})_2$ is well described by the present model as shown in figure 4. The values of the magnetic parameters were least-squares fitted within several assumptions: Mn–Mn super-superexchange interactions through H_2O molecules were neglected or included; value of the Curie temperature fixed. The refined values are reported in table 3. Note that the high temperature limit of the hyperfine field is zero in any case, as shown in figure 4.

There is a rather good agreement between expected and calculated values of the Curie constants and the Curie temperature for each of the assumptions. On the other hand, the values of the magnetic interactions can be discussed with respect to previous data.

(i) $J_{\text{Fe-Fe}}$ was directly deduced from the magnetic susceptibility of isostructural $\text{ZnFeF}_5(\text{H}_2\text{O})_2$, which has only Fe–Fe antiferromagnetic interactions: -11.8 K (Laligant *et al* 1986); this only compares with values obtained here when Mn–Mn interactions are included.

(ii) The ratio of exchange integrals $J_{\text{Mn-Fe}}/J_{\text{Fe-Fe}}$ was deduced from simulations of the magnetic structure (at 0 K), and found to be equal to 0.49 (Lacorre and Pannetier 1987, Lacorre 1988) or 0.40 (Linares *et al* 1988) respectively, neglecting and including the Mn–Mn super-superexchange interactions; the values obtained here are respectively 0.18 and 0.36 so that the assumption of sizable Mn–Mn interactions is again preferred.

Consequently, one can conclude that the Mn–Mn super-superexchange interactions through water molecules are needed for a coherent description of the magnetic properties of the system.

8. Conclusion

High field Mössbauer spectroscopy has successfully measured the specific contribution of the ferric moments to the magnetic susceptibility. This method could be widely applied to isotropic magnetic atoms having a convenient Mössbauer isotope; it is currently being adapted to amorphous insulators where it involves molecular field distributions which cannot be determined accurately by the usual susceptibility measurements.

In addition, the data recorded with $\text{MnFeF}_5(\text{H}_2\text{O})_2$ were analysed in a molecular field model with good results, and yielded a coherent set of magnetic exchange integral values; a peculiarity of this frustrated system is the compensation temperature for the iron-sublattice contribution to the magnetic susceptibility.

Acknowledgments

Acknowledgments are due to Dr Y Laligant, M Leblanc and Professor Ferey for providing us with the samples and to Dr G Czjzek for critical comments during this study.

References

- Chappert J 1974 *J. Physique Coll.* **35** C6 71
Chappert J, Teillet J and Varret F 1979 *J. Magn. Magn. Mater.* **11** 200
Czjzek G 1982 *Phys. Rev. B* **25** 4908
Dezsi I, Kulcsar K, Nagy D L and Pocs L 1971 *Proc. Conf. Appl. Mössbauer (Tihany, 1969)* ed I Dezsi, p 247
Ferey G, de Pape R, Leblanc M and Pannetier J 1986 *Rev. Chim. Minér.* **23** 1974
Greneche J M, Le Bail A, Leblanc M, Mosset A, Galy J, Varret F and Ferey G 1988a *J. Phys. C: Solid State Phys.* **15** 1351
Greneche J M, Linares J, Varret F, Laligant Y and Ferey G 1988b *J. Magn. Magn. Mater.* **73** 115
Greneche J M and Varret F 1988c *Hyperfine Interact.* **42** 935
Heger G and Geller L 1972 *Phys. Status Solidi b* 227
Heger G, Geller L and Babel D 1971 *Solid State Commun.* **9** 335
Herpin A 1968 *Théorie du Magnétisme* (Paris: PUF) p 621
Huynh B H and Kent T A 1983 *Advances in Mössbauer Spectroscopy: Studies in Physical and Theoretical Chemistry* (New York: Elsevier) p 490
Lacorre P 1988 *Thèse de Doctorat Université du Maine*
Lacorre P and Pannetier J 1987 *J. Magn. Magn. Mater.* **71** 63
Laligant Y, Calage Y, Torres-Tapia E, Greneche J M, Varret F and Ferey G 1986 *J. Magn. Magn. Mater.* **61** 283
Le Caer G, Cadogan J M, Brand R A, Dubois J M and Guntherodt H J 1984 *J. Phys. F: Met. Phys.* **14** L73
Linares J, Greneche J M and Varret F 1988 *J. Physique* **49** C8 901
Mariot J P, Guillin J, Varret F, Lauer S and Trautwein A X 1986 *Hyperfine Interact.* **30** 221
Mariot J P, Michaud P, Lauer S, Astruc D, Trautwein A X and Varret F 1983 *J. Physique* **44** 1377
Maurer M, Friedt J M and Sanchez J P 1985 *J. Phys. F: Met. Phys.* **15** 1449
Spartalian K 1983 *Advances in Mössbauer Spectroscopy: Studies in Physical and Theoretical Chemistry* (New York: Elsevier) p 455
Spartalian K and Lang K 1980 *Applications of Mössbauer Spectroscopy* vol II, ed R L Cohen
Varret F 1982 *Int. Conf. Appl. Mössbauer Effect (Jaipur, 1982)* p 129
Varret F, Hamzic A and Campbell I A 1982 *Phys. Rev. B* **26** 5285
Varret F and Jehanno G 1975 *J. Physique* **36** 415